








A conserved molecular logic for neurogenesis to gliogenesis switch in the cerebral cortex

Xiaoyi G. Liang^a, Kendy Hoang^a, Brandon L. Meyerink^{b,c}, Pratiksha Kc^b, Kitt Paraiso^d, Li Wang^{e,f}, Ian R. Jones^g, Yue Zhang^{a,1}, Sol Katzman^h , Thomas S. Finn^a , Jeremiah Tsyporin^a, Fangyuan Qu^a, Zhaoxu Chen^a , Axel Visel^{d,i,j}, Arnold Kriegstein^{e,f} , Yin Shen^{f,g}, Louis-Jan Pilaz^{b,c}, and Bin Chen^{a,2} 

Edited by Nenad Sestan, Yale University School of Medicine, New Haven, CT; received December 20, 2023; accepted April 2, 2024 by Editorial Board Member Jeremy Nathans

During development, neural stem cells in the cerebral cortex, also known as radial glial cells (RGCs), generate excitatory neurons, followed by production of cortical macroglia and inhibitory neurons that migrate to the olfactory bulb (OB). Understanding the mechanisms for this lineage switch is fundamental for unraveling how proper numbers of diverse neuronal and glial cell types are controlled. We and others recently showed that Sonic Hedgehog (Shh) signaling promotes the cortical RGC lineage switch to generate cortical oligodendrocytes and OB interneurons. During this process, cortical RGCs generate intermediate progenitor cells that express critical gliogenesis genes *Ascl1*, *Egfr*, and *Olig2*. The increased *Ascl1* expression and appearance of *Egfr*⁺ and *Olig2*⁺ cortical progenitors are concurrent with the switch from excitatory neurogenesis to gliogenesis and OB interneuron neurogenesis in the cortex. While Shh signaling promotes *Olig2* expression in the developing spinal cord, the exact mechanism for this transcriptional regulation is not known. Furthermore, the transcriptional regulation of *Olig2* and *Egfr* has not been explored. Here, we show that in cortical progenitor cells, multiple regulatory programs, including *Pax6* and *Gli3*, prevent precocious expression of *Olig2*, a gene essential for production of cortical oligodendrocytes and astrocytes. We identify multiple enhancers that control *Olig2* expression in cortical progenitors and show that the mechanisms for regulating *Olig2* expression are conserved between the mouse and human. Our study reveals evolutionarily conserved regulatory logic controlling the lineage switch of cortical neural stem cells.

gliogenesis | neurogenesis | lineage switch | enhancer | *Olig2*

The production of proper numbers of diverse neurons and macroglia by neural stem cells (NSCs) is essential for neural circuit formation and brain function. During development, NSCs in the cerebral cortex, known as radial glial cells (RGCs), generate glutamatergic neurons that populate different cortical layers (1). As the generation of excitatory neurons ceases, cortical RGCs switch lineages and generate oligodendrocytes, astrocytes, and GABAergic olfactory bulb (OB) interneurons (2–6). Proper control of this lineage switch ensures the production of diverse neuronal and glial cell types in correct numbers.

The lineages of cortical RGCs have been under extensive scrutiny. Results from cell transplant studies using ferret and rat models suggested that early cortical progenitors are multipotent and sequentially generate diverse excitatory neuron subtypes that populate the cortical layers in an inside-out pattern (1). These results were supported by clonal analysis of individually cultured cortical progenitors (7). A later study reported that early (embryonic day 10.5, or E10.5) *Cux2*-expressing (*Cux2*⁺) cortical RGCs were intrinsically lineage-restricted to generate later-born corticocortical projection neurons (8). However, through in vivo lineage analyses of individual RGCs, it was found that early RGCs, including the *Cux2*⁺ RGCs, are multipotent, and they sequentially generate diverse subtypes of cortical excitatory neurons, followed by OB interneurons and macroglia (2, 9–11).

How is the lineage progression of cortical RGCs regulated to ensure distinct neuronal and glial progenies are generated at different times? By labeling cortical RGCs at the end of excitatory neuron production in mice and performing single-cell RNA-seq analysis of the labeled progeny, Li et al. reported that some late cortical RGCs become translocating RGCs and migrate away from the VZ into the cortical plate to produce astrocytes (12). Other late RGCs remain at the VZ. They divide and generate transient multipotent intermediate progenitors (MIPCs) that are marked by the coexpression of *Ascl1*, *Egfr*, and *Olig2*. These *Ascl1*⁺*Egfr*⁺*Olig2*⁺ MIPCs further divide and generate the progenitors for cortical astrocytes, oligodendrocytes, and inhibitory interneurons that migrate to the

Significance

In the developing cerebral cortex, neural stem cells switch from generating cortical excitatory neurons to producing cortical glia and olfactory bulb interneurons. This lineage switch is essential for generating appropriate numbers of neuronal and glial cell types in the cortex and requires the transcription of *Olig2* in cortical progenitors. In this study, we describe the identification of multiple enhancers that control the expression of *Olig2* in cortical progenitors using ChIP-seq, CUT&RUN, ATAC-seq, enhancer reporter, and deletion mice. Our study reveals a conserved mechanism for *Olig2* gene expression and neural stem cell lineage regulation between the mouse and human.

Author contributions: X.G.L., K.H., K.P., L.W., I.R.J., Y.Z., A.V., A.K., Y.S., L.-J.P., and B.C. designed research; X.G.L., K.H., B.L.M., P.K., K.P., L.W., I.R.J., Y.Z., T.S.F., J.T., F.Q., Z.C., L.-J.P., and B.C. performed research; X.G.L., K.H., K.P., L.W., I.R.J., S.K., and B.C. analyzed data; and X.G.L. and B.C. wrote the paper.

The authors declare no competing interest.

This article is a PNAS Direct Submission. N.S. is a guest editor invited by the Editorial Board.

Copyright © 2024 the Author(s). Published by PNAS. This open access article is distributed under [Creative Commons Attribution License 4.0 \(CC BY\)](https://creativecommons.org/licenses/by/4.0/).

¹Present address: Children's Hospital, National Clinical Research Center for Child Health & Liangzhu Laboratory, Zhejiang University School of Medicine, Hangzhou 310000, China.

²To whom correspondence may be addressed. Email: bchen@ucsc.edu.

This article contains supporting information online at <https://www.pnas.org/lookup/suppl/doi:10.1073/pnas.2321711121/-DCSupplemental>.

Published May 7, 2024.

OB (4, 12). Immunohistochemical analysis of embryonic mouse and fetal human brains confirms the presence of $Ascl1^+Egfr^+Olig2^+$ MIPCs in cortical ventricular and subventricular zones (V/SVZ), which give rise to intermediate progenitors for both cortical macroglia and the OB interneurons (4, 12, 13).

Expression of $Ascl1$, $Egfr$, and $Olig2$ is critical for the lineage switch of cortical RGCs. $Ascl1$ has been reported to be essential for gliogenesis in both the spinal cord and telencephalon (14–16). It is expressed in cortical progenitors from the beginning of cortical neurogenesis (17). Recent elegant studies have shown that $Egfr$ critically regulates cortical gliogenesis in a region-specific pattern (5, 6). During development, it is initially expressed in ventral forebrain progenitors, but its expression is turned on in cortical progenitors around E16.5 in mice, coincident with the onset of cortical RGC lineage switch (12).

$Olig2$ encodes a basic helix–loop–helix (bHLH) transcription factor that is required for the specification of oligodendrocyte precursor cells (OPCs) and differentiation of oligodendrocytes (18–21). Previous studies have shown that $Olig2$ is also expressed in developing astrocytes and plays a pivotal role in their development (21). Among the forebrain progenitors, $Olig2$ is initially expressed in the NSCs located in the medial ganglionic eminence. At E16.5, when the production of excitatory neurons ceases, $Olig2$ expression starts to be detected in cortical progenitor cells in the subventricular zone (SVZ), and this expression persists into early postnatal stages (12). Intersectional lineage analysis indicated that in addition to the oligodendrocytes, the $Olig2^+$ cortical progenitors give rise to almost all cortical astrocytes and some OB interneurons (12). Indeed, cortex-specific deletion of $Olig2$ leads to defective production of both cortical oligodendrocytes and astrocytes (21). However, the molecular mechanism underlying the onset of $Olig2$ expression in cortical progenitors has not been determined.

We and others reported that Shh signaling is both necessary and sufficient to promote cortical RGCs to generate OB interneurons and oligodendrocytes (4, 22). We found that Shh signaling activates this lineage switch by causing the degradation of the transcription repressor $Gli3$ (4). Here, we report that $Gli3$ and $Pax6$, transcription factors highly expressed in the cortical RGCs, prevent precocious expression of $Olig2$ and the lineage switch of cortical RGCs. We identify multiple *cis*-regulatory sequences that are recruited to the $Olig2$ promoter and promote $Olig2$ transcription in cortical progenitor cells. We show that these regulatory sequences are conserved in the human genome and are recruited to the $OLIG2$ promoter in cortical progenitors in the human prenatal brain. Thus, we have identified a conserved molecular mechanism that promotes $Olig2/OLIG2$ expression and a cortical neural stem cell lineage switch in the mouse and human.

Results

Shh Signaling Promotes the Generation and Proliferation of $Ascl1^+Egfr^+$ and $Egfr^+Olig2^+$ Intermediate Progenitors (IMPs) in the Cortical VZ/SVZ. As cortical RGCs undergo the lineage switch to generate OB interneurons and cortical glia, they generate IMPs for these lineages that can be identified by coexpression of $Ascl1$, $Egfr$, and $Olig2$ (12, 13). We and others reported that Shh signaling is essential for cortical RGCs to produce oligodendrocytes and OB interneurons (4, 22). To determine how Shh signaling regulates this lineage switch, we deleted the Shh receptor and signaling transducer, *Smoothed* (*Smo*), in late cortical RGCs and examined the expression of $Ascl1$, $Egfr$, and $Olig2$ in the cortical SVZ of control ($Smo^{fl/+}$) and *hGFAP-Cre*; $Smo^{fl/fl}$ (*Smo cko*) mice (23). Since both $Ascl1$ and $Olig2$ antibodies were made in rabbits, we examined the $Ascl1^+Egfr^+$

and $Egfr^+Olig2^+$ IMPs. In the control brains, the $Ascl1^+Egfr^+$ and $Egfr^+Olig2^+$ IMPs were initially observed at E16.5, and their numbers continued to increase until birth (Fig. 1 *A–C* and *G–I*). In the *Smo cko* brains however, expression of $Ascl1$ was reduced, and $Egfr$ and $Olig2$ expressions were absent in the cortical VZ/SVZ at E16.5. $Ascl1^+Egfr^+$ and $Egfr^+Olig2^+$ cortical IMPs were observed from E17.5, but, compared to the control brains, the numbers of $Ascl1^+Egfr^+$ and $Egfr^+Olig2^+$ cells were significantly reduced (Fig. 1 *D–F* and *J–N*). Thus, blocking Shh signaling leads to delayed appearance and reduced numbers of $Ascl1^+Egfr^+$ and $Egfr^+Olig2^+$ IMPs, which give rise to cortical glia and some OB interneurons.

To examine whether Shh signaling regulates the proliferation of these IMPs, we injected EdU at E17.5 to label S phase cells and collected the brains 2 h later (*SI Appendix*, Fig. S1). We found that, compared to littermate $Smo^{fl/+}$ control mice, the numbers of EdU^+ , EdU^+Olig2^+ , EdU^+Ascl1^+ , EdU^+Egfr^+ , $EdU^+Ascl1^+Egfr^+$, and $EdU^+Olig2^+Id1^+$ cells in the VZ/SVZ of *Smo cko* mice were significantly reduced (*SI Appendix*, Fig. S1 *A–Q*, *S–W*, and *Y*). The numbers of $Ki67^+$ cells were also reduced (*SI Appendix*, Fig. S1 *R*, *X*, and *Y*). Quantification of the percentages of $Ascl1^+$, $Egfr^+$, and $Olig2^+$ cells that were labeled by EdU indicated that lower percentages of $Ascl1^+$ and $Olig2^+$ progenitor cells were in S phase in the *Smo cko* mice (*SI Appendix*, Fig. S1 *Y*). This indicates that in addition to promoting cortical RGCs to generate the IMPs for the macroglial and OB interneuron lineages, Shh signaling promotes the proliferation of these IMPs.

$Olig2$ Is Essential for Cortical RGCs to Generate Oligodendrocytes, Astrocytes, and Olfactory Bulb Interneurons. Lineage analysis of the $Olig2^+$ cortical progenitors showed that they give rise to oligodendrocytes, all cortical astrocytes, and some OB interneurons (12). We examined the function of $Olig2$ in the lineage switch of cortical RGCs by analyzing the $Olig2^{-/-}$ mice (24) at E18.5 (Fig. 2), immediately before their neonatal death. No $Sox10^+$ oligodendrocyte precursors (OPCs) and oligodendrocytes were observed in the cortices of $Olig2^{-/-}$ mice (Fig. 2 *B* and *G*), consistent with its essential role in oligodendrocyte development. Compared to the wild-type cortices, we did not observe significant changes in the numbers of $Ascl1^+$ and $Egfr^+$ cells in the SVZ (Fig. 2 *C*, *D*, *H*, *I*, and *U*), indicating that the generation of $Ascl1^+$ and $Egfr^+$ IMPs do not depend on $Olig2$.

The mitogen-activated protein kinase (MAPK) pathway is essential for gliogenesis in the developing cortex (25). We examined the numbers of activated/phosphorylated $MAPK^+$ cells in the SVZ and found that they were not significantly affected in the $Olig2^{-/-}$ mice at E18.5 (Fig. 2 *E*, *J*, and *U*), consistent with $Olig2$ expression being downstream of MAPK pathway (25). The numbers of the $Olig1^+$ and $Sox9^+$ glial progenitors in the cortical plate were significantly reduced in the absence of $Olig2$ (Fig. 2 *K*, *L*, *P*, *Q*, and *U*). $Id1$ and $Aldh111$ are expressed in RGCs in the VZ, IMPs in the SVZ, as well as astrocyte precursors and astrocytes in the cortical plate. Both $Id1^+$ and $Aldh111^+$ cells were significantly reduced in the SVZ and the cortical plate of $Olig2^{-/-}$ mice (Fig. 2 *M*, *N*, *R*, *S*, and *U*). While the numbers of $Sp8^+$ cortical interneurons were not affected, the numbers of $Sp8^+$ olfactory bulb interneuron neuroblasts in the SVZ were significantly reduced in the $Olig2^{-/-}$ mice (Fig. 2 *O*, *R*, and *U*). Thus, in addition to oligodendrocytes, $Olig2$ is required for cortical RGCs to generate proper numbers of astrocyte progenitors and olfactory bulb interneurons.

$Gli3$ Inhibits $Olig2$ Expression in the Cortical Progenitor Cells. We recently showed that Shh signaling promotes the lineage switch of cortical RGCs by causing the degradation of transcription repressor

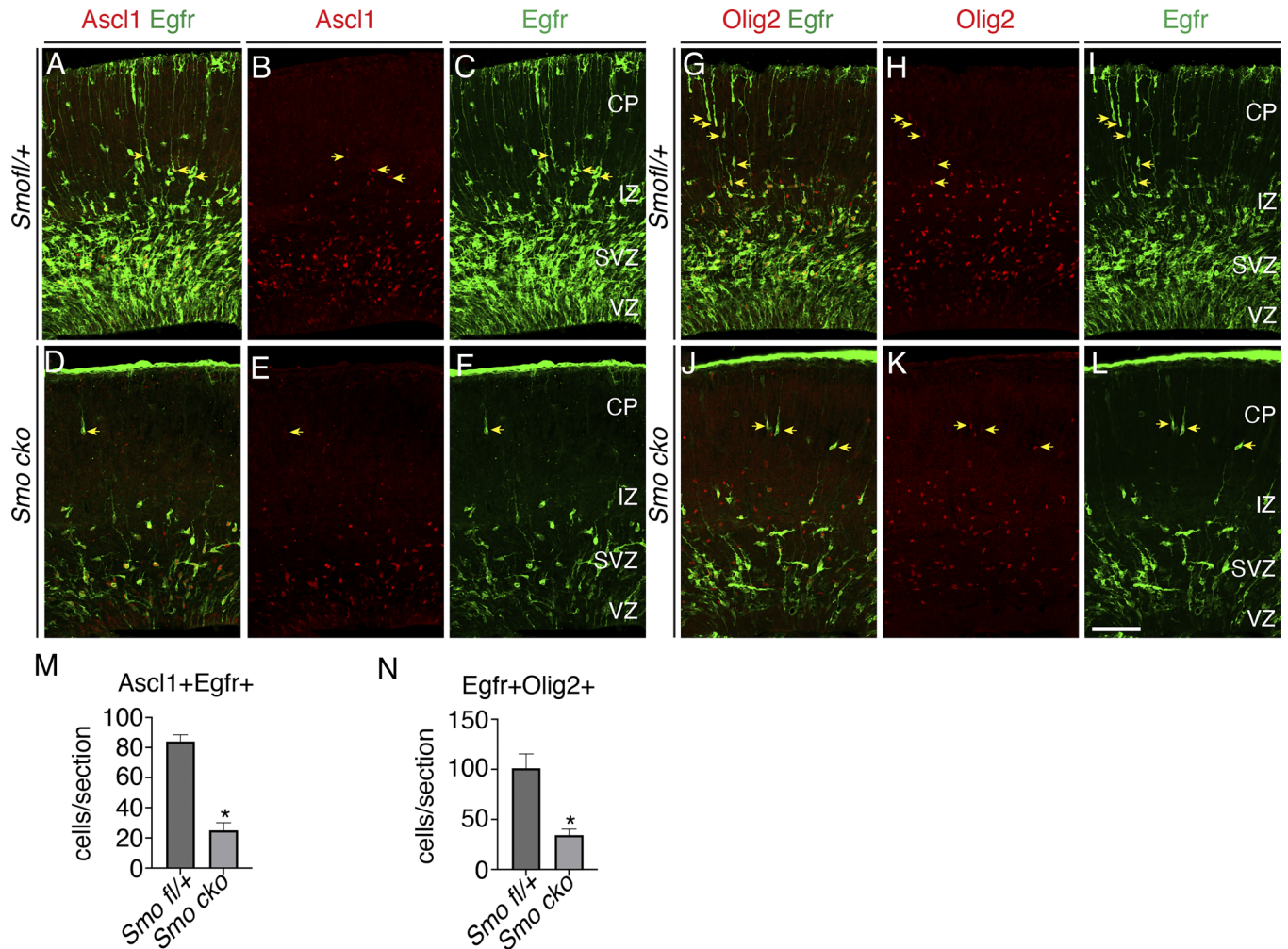


Fig. 1. Fewer $Ascl1^{+}Egfr^{+}$ and $Egfr^{+}Olig2^{+}$ IMPs were present in the cortical VZ/SVZ of E17.5 *Smo cko* mice. (A–L) Immunostaining for *Ascl1*, *Egfr*, and *Olig2* in *Smo^{fl/+}* (A–C and G–I) and *Smo cko* cortices (D–F and J–L). Images were taken at the rostral-middle position along the rostral-caudal axis. (M and N) Quantification of the $Ascl1^{+}Egfr^{+}$ and $Egfr^{+}Olig2^{+}$ cells. Numbers represent means + SEM (n = 3 mice per genotype). * $P < 0.05$; unpaired Student's *t* test. (Scale bars: 100 μ m in L, applies to A–L.)

Gli3 (4). To determine the molecular mechanism underlying *Olig2* expression in cortical progenitor cells, we examined *Gli3* and *Olig2* protein expression in the cortical VZ/SVZ at P0 using immunohistochemistry and western blot analysis (SI Appendix, Fig. S2). Cell density did not change in *Smo cko* mice (SI Appendix, Fig. S2 G, K, O, and S). In the *Smo cko* mice, more cells expressed *Gli3* (SI Appendix, Fig. S2 E, I, M, and Q), and the number of *Olig2*⁺ progenitor cells in the cortical VZ/SVZ was reduced (SI Appendix, Fig. S2 F, J, N, and R). Compared to the wild-type cells, *Gli3* protein in the *Smo cko* cortical progenitors shows a distribution that is significantly skewed toward higher expression (SI Appendix, Fig. S2A), and the *Olig2* protein is significantly skewed toward lower expression (SI Appendix, Fig. S2B). Quantification of fluorescence levels shows a negative correlation between *Gli3* and *Olig2* expression in both wild-type and *Smo cko* VZ/SVZ cortical progenitor cells (SI Appendix, Fig. S2C), suggesting that *Gli3* inhibits *Olig2* expression. Western blot showed that compared to the wild-type cortices, the ratio of *Gli3* repressor (*Gli3R*) to the activator (*Gli3A*) in the P0 *Smo cko* cortices was significantly increased (SI Appendix, Fig. S2 T and U), further supporting *Shh* signaling promotes *Olig2* expression by decreasing *Gli3R*.

***Gli3* and *Pax6* Regulate OB Interneuron Production from Cortical Progenitors Combinatorially.** *Pax6* is highly expressed in cortical RGCs. Its expression in glial progenitors of the neonatal SVZ

represses *Olig2* expression and induces a neurogenic fate (26). To determine whether *Pax6* regulates gliogenesis and OB interneuron production and to circumvent the early requirement of *Pax6* in regulating the dorsal–ventral patterning of the telencephalon (27), we examined the brains of E16.5 and P0 *hGFAP-Cre; Pax6^{fl/fl}* and *Emx1-Cre; Pax6^{fl/fl}* mice (SI Appendix, Fig. S3). Immunostaining with cortical projection neuron markers *Ctip2* and *Satb2* indicated that dorsal–ventral patterning of the telencephalon occurred normally in these mice (SI Appendix, Fig. S3 P–U). Compared to the wild-type mice, significantly more *Olig2*⁺, *Gsx2*⁺, and *Sp8*⁺ cells, and fewer *Tbr2*⁺ excitatory neuron progenitors were present in the VZ/SVZ of E16.5 *hGFAP-Cre; Pax6^{fl/fl}* and *Emx1-Cre; Pax6^{fl/fl}* cortices (SI Appendix, Fig. S3 A–O and V), indicating that similar to *Gli3* (4), *Pax6* promotes excitatory neuron lineage, and inhibits cortical RGCs from generating glia and OB interneurons. At P0, while *Gsx2*⁺ cortical progenitors and *Sp8*⁺ OB interneuron neuroblasts remained increased in the *hGFAP-Cre; Pax6^{fl/fl}* mice (Fig. 3 B, C, F, G, and Q), the number of *Olig2*⁺ cells in the cortical VZ/SVZ was no longer significantly increased (Fig. 3 A, E, and Q), likely due to the inhibition by high-level *Gsx2* expression.

The similar lineage defects in the VZ/SVZ of *hGFAP-Cre; Pax6^{fl/fl}* (SI Appendix, Fig. S3) and the *hGFAP-Cre; Gli3^{fl/fl}* mice (4) indicate that both *Pax6* and *Gli3* inhibit cortical RGCs to generate olfactory bulb interneurons and cortical glia. To investigate whether they act synergistically, we analyzed brains from P0

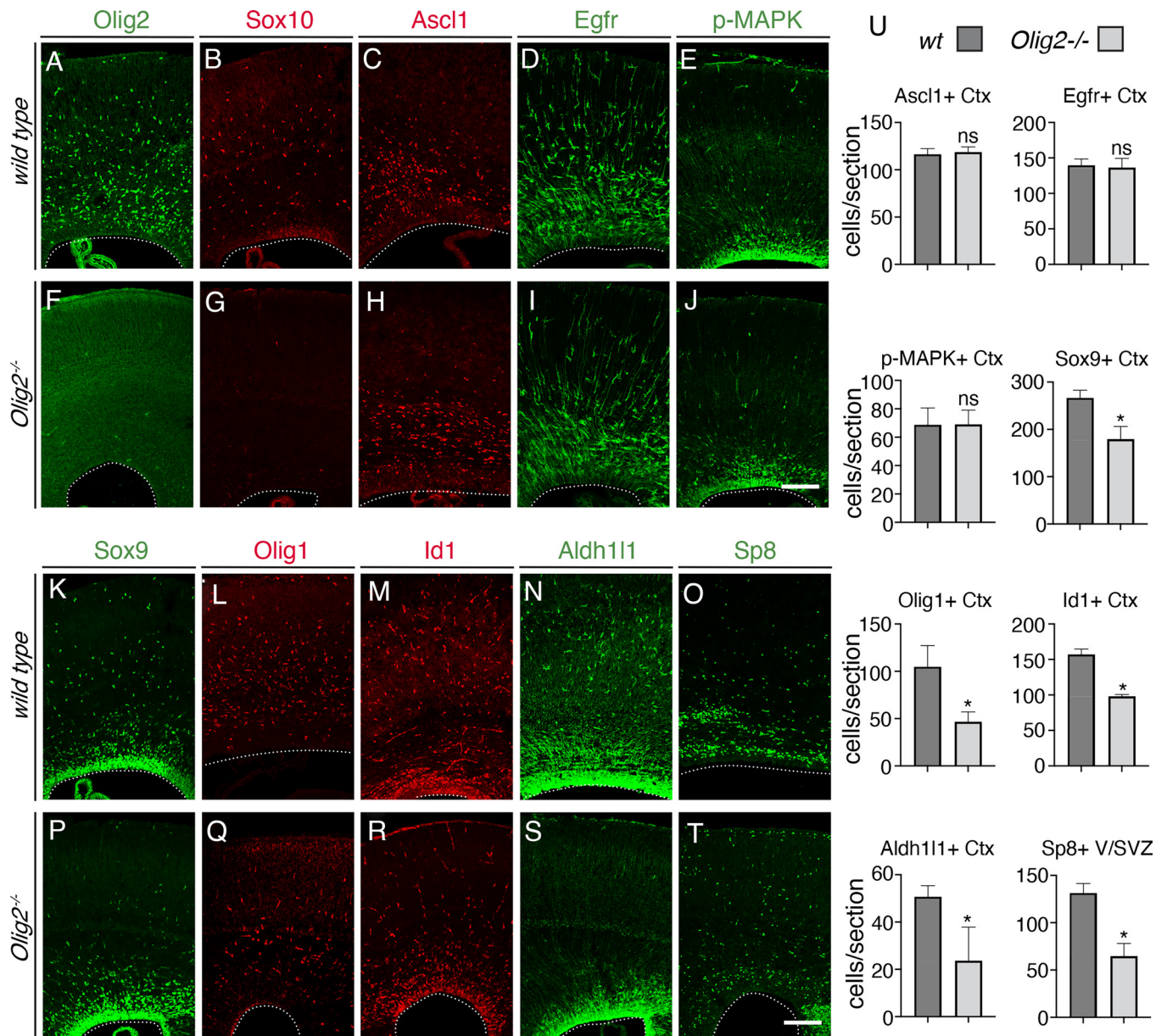


Fig. 2. *Olig2* deletion leads to fewer cells of oligodendrocyte, astrocyte, and olfactory bulb interneuron lineages at E18.5. (A–T), Immunostaining for *Olig2* (A and F), *Sox10* (B and G), *Ascl1* (C and H), *Egfr* (D and I), phosphorylated MAPK (E and J), *Sox9* (K and P), *Olig1* (L and Q), *Id1* (M and R), *Aldh111* (N and S), and *Sp8* (O and T) in wild-type (A–E and K–O) and *Olig2*^{-/-} (F–J and P–T) cortices. Images were taken at the rostral-middle position along the rostral-caudal axis. (U) Quantification of *Ascl1*⁺, *Egfr*⁺, phosphorylated MAPK⁺, *Sox9*⁺, *Olig1*⁺, *Id1*⁺, *Aldh111*⁺, and *Sp8*⁺ cells. Numbers represent means + SEM (n = 3 mice per genotype). *P < 0.05; unpaired Student's *t* test. (Scale bars: 100 μm in J and T, applies to A–J and K–T, respectively).

hGFAP-Cre; Gli3^{fl/+}; Pax6^{fl/+} and *hGFAP-Cre; Gli3^{fl/fl}; Pax6^{fl/fl}* mice (Fig. 3). Neither *hGFAP-Cre; Gli3^{fl/+}* nor *hGFAP-Cre; Pax6^{fl/+}* mice showed changes in the *Olig2*⁺, *Gsx2*⁺, or *Sp8*⁺ cells in the cortical VZ/SVZ. Compared to the wild-type mice (Fig. 3 A–C), the numbers of *Olig2*⁺ cortical progenitor cells were not significantly affected, but the numbers of *Gsx2*⁺ cortical progenitor cells and the *Sp8*⁺ OB interneuron neuroblasts were significantly increased in the cortical VZ/SVZ of P0 *hGFAP-Cre; Gli3^{fl/+}; Pax6^{fl/+}* mice (Fig. 3 I–K and Q). In the P0 *hGFAP-Cre; Gli3^{fl/fl}; Pax6^{fl/fl}* brains, the numbers of *Gsx2*⁺ IMPs in the cortical VZ/SVZ were not significantly different from those in the *hGFAP-Cre; Pax6^{fl/fl}* and the *hGFAP-Cre; Gli3^{fl/fl}* mice, but the number of the *Sp8*⁺ OB interneuron neuroblasts drastically increased (Fig. 3 M–O and Q). These results indicate that *Gli3* and *Pax6* function in parallel to inhibit cortical RGCs from generating OB interneuron lineage. Consistent with this, protein coimmunoprecipitation with either

a *Gli3* antibody or a *Pax6* antibody did not pull down the other protein.

Identification of Genome-wide *Gli3* Binding Sites in the Cortical Cells.

To determine whether *Gli3* inhibits *Olig2* expression directly, we performed chromatin-immunoprecipitation (ChIP) and Cleavage Under Targets & Release Using Nuclease (CUT&RUN) using a *Gli3* antibody and dissected E15 cortical tissues, followed by high-throughput DNA sequencing (28). The results were highly consistent both within and between the ChIP-seq and CUT&RUN experiments (n = 3 for each experiment). Both ChIP and CUT&RUN showed the specific binding of *Gli3* to promoters and enhancers of *Shh* target genes such as *Gli1* and *Ptch1* (SI Appendix, Fig. S4). We identified 4,414 *Gli3* binding sites (GBS) in the ChIP-seq experiments using irreproducible discovery rate (IDR) analysis (29). The GBS are located in both promoter and nonpromoter regions (SI Appendix, Fig. S5A).

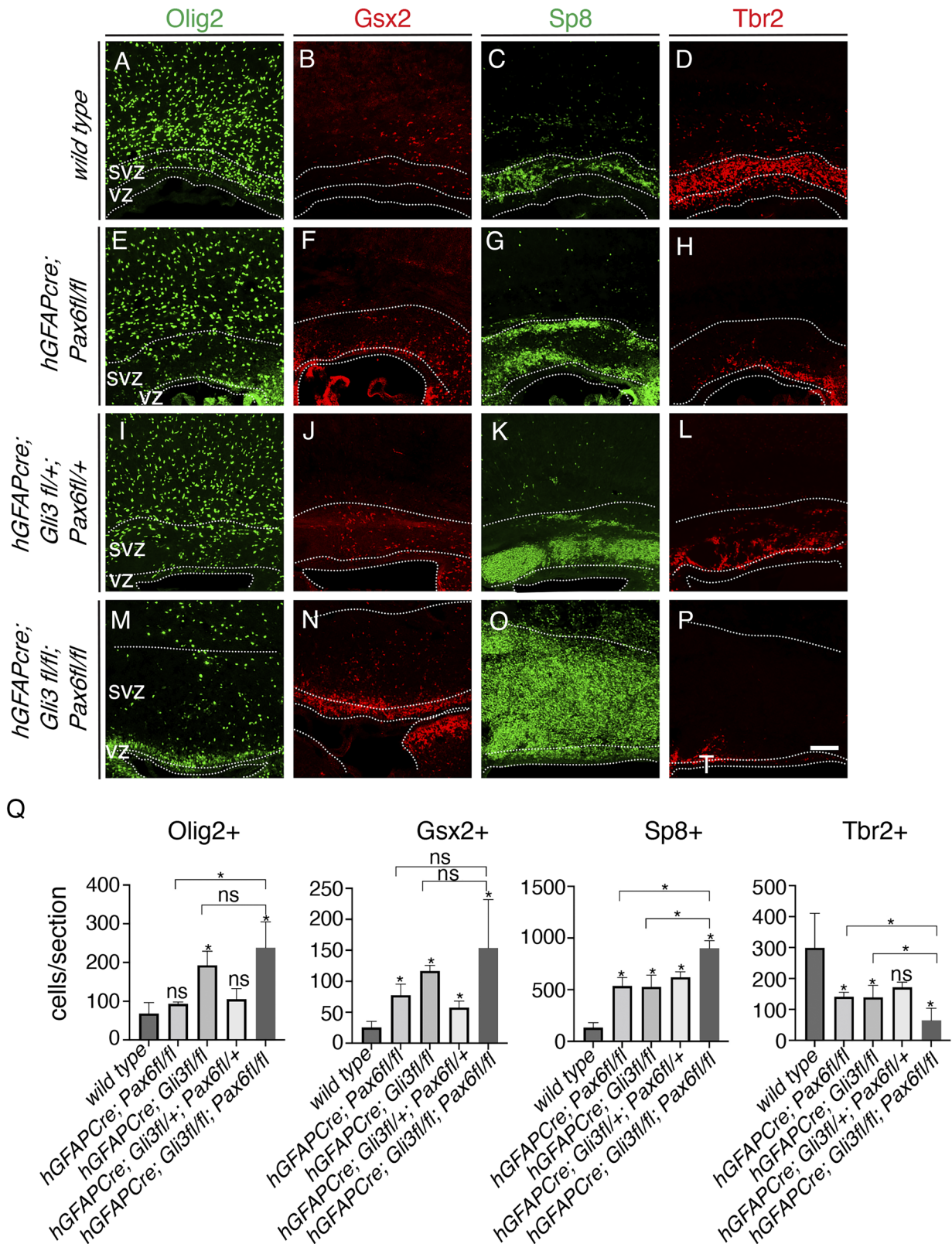


Fig. 3. Pax6 and Gli3 repress olfactory bulb interneuron lineage. (A–P), Immunostaining of Olig2 (A, E, I, and M), Gsx2 (B, F, J, and N), Sp8 (C, G, K, and O), and Tbr2 (D, H, L, and P) in the cortices of P0 wild-type (A–D), hGFAPCre; Pax6^{fl/fl} (E–H), hGFAPCre; Gli3^{fl/fl}; Pax6^{fl/+} (I–L), and hGFAPCre; Gli3^{fl/fl}; Pax6^{fl/fl} (M–P) mice. Images were taken at the rostral-middle position along the rostral-caudal axis. (Q) Quantification of Olig2⁺, Gsx2⁺, Sp8⁺, and Tbr2⁺ cells in 300-μm wide VZ/SVZ regions. Dotted lines demarcate the VZ and SVZ. Numbers represent means + SEM (n = 3 mice per genotype). ns, not significant; *P < 0.05; unpaired Student's t test. (Scale bar: 100 μm in P, applies to A–P.)

We identified the motifs enriched in the GBS at the promoter and nonpromoter regions using the MEME-ChIP online tool, and the most significantly enriched motifs were the known consensus Gli binding sequences (SI Appendix, Fig. S5B).

To determine whether the GBS were potential promoters or enhancers, we performed CUT&RUN for H3K27me3, H3K27ac, and H3K4me3 using E15 and E16 cortices. We intersected the GBS at promoter [from transcription start site (TSS) and up to 2 kb

upstream] regions and nonpromoter [more than 2 kb away from the TSS] regions, with the binding sites for H3K27me₃, H3K27ac, and H3K4me₃ revealed in our CUT&RUN data. We found that the GBS at both the promoter and nonpromoter regions were enriched with these histone modifications (SI Appendix, Fig. S5 C and D), indicating that the identified GBS are likely active promoters and enhancers.

Gli3 and Pax6 Bind to Conserved Sequences in the *Olig1/2* Loci.

Olig2 and its close homolog *Olig1* are located 36 kb apart on chromosome 16 in the mouse genome. ChIP-seq revealed 3 GBS in highly conserved nonpromoter regions (Fig. 4A and SI Appendix, Fig. S6). GBS1 was within the predicted ENCODE (30–32) enhancer e14414 in brain tissue, and GBS3 overlapped with predicted enhancer e14416 (Fig. 4A). GBS2 and GBS3 exhibited enrichment of H3K27me₃ and H3K4me₃ (SI Appendix, Fig. S6). To further investigate whether these GBS are potential enhancers, we performed CUT&RUN for H3K27me₃ and H3K4me₃ using dissected cortices from E16.5 control (*RosaSmoM2*), or *hGFAP-Cre; RosaSmoM2* mice, the latter of which express a constitutively activated Smoothed protein and exhibit increased Shh signaling in cortical progenitor cells (4). We previously showed increased numbers of *Olig2*⁺ cortical progenitors and OB interneuron lineage cells in the VZ/SVZ of *hGFAP-Cre; RosaSmoM2* mice (4). We observed increased H3K4me₃ at GBS1 and GBS3, and reduced H3K27me₃ at GBS2 in the *hGFAP-Cre; RosaSmoM2* cells (SI Appendix, Fig. S6). In addition, we coelectroporated *pCAG-ShhN* and *pCAG-Cre* plasmids or *pCAG-Cre* plasmids alone into the cortical VZ of E13.5 *Rosa26^{RCE-GFP}* reporter mice to label late cortical RGCs, and enriched for the GFP⁺ cells at E16.5 using fluorescence activate cell sorting (FACS). We performed Assay of Transposase Accessible Chromatin sequencing (ATAC-seq) on the sorted cells, and observed increased accessibility at both *Olig1* and *Olig2* genes, as well as the 3 GBS in the cells from the brain electroporated with *pCAG-ShhN* plasmids (SI Appendix, Fig. S6), confirming Shh signaling promotes the accessibility of *Olig1/2* genes and these GBS. To determine whether *Olig1* or *Olig2* promoters could be regulated by these GBS, we performed a 4C experiment (33), a derivative of chromatin conformation capture (3C), using the promoter sequences of *Olig1* and *Olig2* as baits to capture their interacting sequences. We found that all 3 GBS interacted with these promoters in the cortical cells (Fig. 4A), suggesting a direct regulatory relationship.

The *hGFAP-GFP* transgenic mouse line expresses GFP under the control of the human GFAP promoter in cortical RGCs, and the GFP proteins carry over from RGCs to their immediate progeny (34). We mined the single-cell ATAC-seq (scATAC-seq) data of 4721 *hGFAP-GFP*⁺ cortical cells enriched by FACS from E18.5 *hGFAP-GFP* mice (12), and analyzed chromatin accessibility in the clusters of RGCs, MIPCs, projection neuron lineage, astrocyte lineage, oligodendrocyte lineage, and OB interneuron lineage (figure 8 in ref. 12). We found that the 3 GBS overlapped with the scATAC-seq peaks that were differentially accessible in different cell types/lineages (Fig. 4B), further suggesting that the GBS are likely enhancers for the *Olig1/2* genes.

To investigate how Pax6 regulates *Olig2* expression, we examined the previously published Pax6 ChIP-seq data (35) and found that Pax6 bound to several regions in the *Olig1/2* loci, including GBS1/e14414, GBS3/e14416, e14412, and e14415 (Fig. 4A). 4C experiments showed that the Pax6 binding sites (PBS) interacted with the *Olig1/2* promoters in the cortical cells (Fig. 4A). Thus, our results demonstrate that Pax6 directly represses *Olig1/2* expression in cortical progenitors.

Gli3 Binding Sites near the *Olig1/2* Loci Show Enhancer Activity in the Developing Cerebral Cortex.

We tested whether the Gli3 and Pax6 binding sites near the *Olig1/2* loci are potential enhancers by examining the Vista Enhancer Browser (36) and generating additional reporter mice (36–38). β -galactosidase (LacZ) expression was assayed in the E11.5 or E16.5 embryos (Fig. 4C). The activity of the human homologous sequence (hs1548) for predicted enhancer e14412 was previously assayed by the Vista Enhancer project, and showed low but consistent (6/6) activity in the forebrain of E11.5 embryos (Fig. 4C). We assayed the activity of both the mouse GBS1/e14414 enhancer (mm817 in Fig. 4C) and the human homologous sequence (hs1188). Both the mouse and human sequences drove high and consistent expression of LacZ in the forebrain, midbrain, hindbrain, and the neural tube (Fig. 4C). 4C experiment showed that the Pax6 binding site between e14412 and e14414 interacted with the *Olig1/2* promoters (PBS in Fig. 4A). We found that the PBS was active in the forebrain and neural tube in the E16.5 mouse embryos (mm2287 in Fig. 4C). We observed LacZ activities in the forebrain, midbrain, neural tube, and limb for the GBS3/e14416 enhancer (mm2289) at E16.5, while e14415 (mm2288) showed activities in the hindbrain, neural tube, and the abdomen at E16.5 (Fig. 4C). Thus, most of the Gli3 and Pax6 binding sites at the *Olig1/2* loci showed enhancer activity in the developing brain.

Gli3 and Pax6 Binding Sites Are Conserved in the Human Genome and Are Recruited to the *OLIG1* and *OLIG2* Promoters in the Cortical Glial Lineages.

During human prenatal brain development, cortical radial glial cells (RGCs) generate macroglia and OB interneurons via *OLIG2*-expressing IMPs (13). We characterized *cis*-regulatory chromatin interactions for RGCs and glial progenitors in fetal cortices. Briefly, we isolated cortical cells from gestation week 15 (GW15) and GW22 human cortices. These cells were dissociated, permeabilized, and stained with markers SOX2, HOPX, OLIG2, and PU.1 to allow type-specific cell isolation via fluorescence-activated cell sorting (FACS). Specifically, we targeted ventricular radial glia (vRG, SOX2⁺HOPX^{low}), outer radial glia (oRG, SOX2⁺HOPX^{high}), glial progenitors (IMP/OPC/oligodendrocytes, OLIG2⁺), and microglia (PU.1⁺). Following cell sorting, we performed H3K4me₃ proximity ligation-assisted ChIP-seq (PLAC-seq) using sorted cells, and applied the Model-based Analysis of PLAC-seq (MAPS) pipeline to call significant H3K4me₃-mediated chromatin interactions at a resolution of 2 kb (39). To determine whether the Gli3 and Pax6 binding sites identified in the cortical progenitor cells in the mouse are potential enhancers for the human *OLIG1/2* genes in cortical progenitors, we identified the human homologous sequences for these binding sites using the Basic Local Alignment Search Tool (40). We examined H3K4me₃ PLAC-seq data and found that human homologous sequences for the e14412, GBS1/e14414, e14415, GBS2, GBS3/e14416, and the PBS interact with *OLIG2* or *OLIG1* promoters (Fig. 4D). Reporter assays showed that the human hs1188 enhancer, which is homologous to the GBS1/e14414, drives high lacZ expression in the E11.5 mouse cortex (Fig. 4C), suggesting that the molecular mechanism for activating *OLIG2* expression in cortical progenitor cells is conserved between the mouse and human.

GBS1/e14414 and GBS2 Are Essential for *Olig2* Expression in Cortical Progenitors and Gliogenesis.

To determine whether the Gli3 and Pax6 binding sites are necessary for *Olig2* expression in cortical progenitor cells, we generated mice carrying deletion alleles for GBS1/e14414, e14415, GBS2, and GBS3/e14416 using a CRISPR-Cas9 strategy (SI Appendix, Fig. S7). We analyzed P0 brains from homozygous enhancer deletion mutant mice

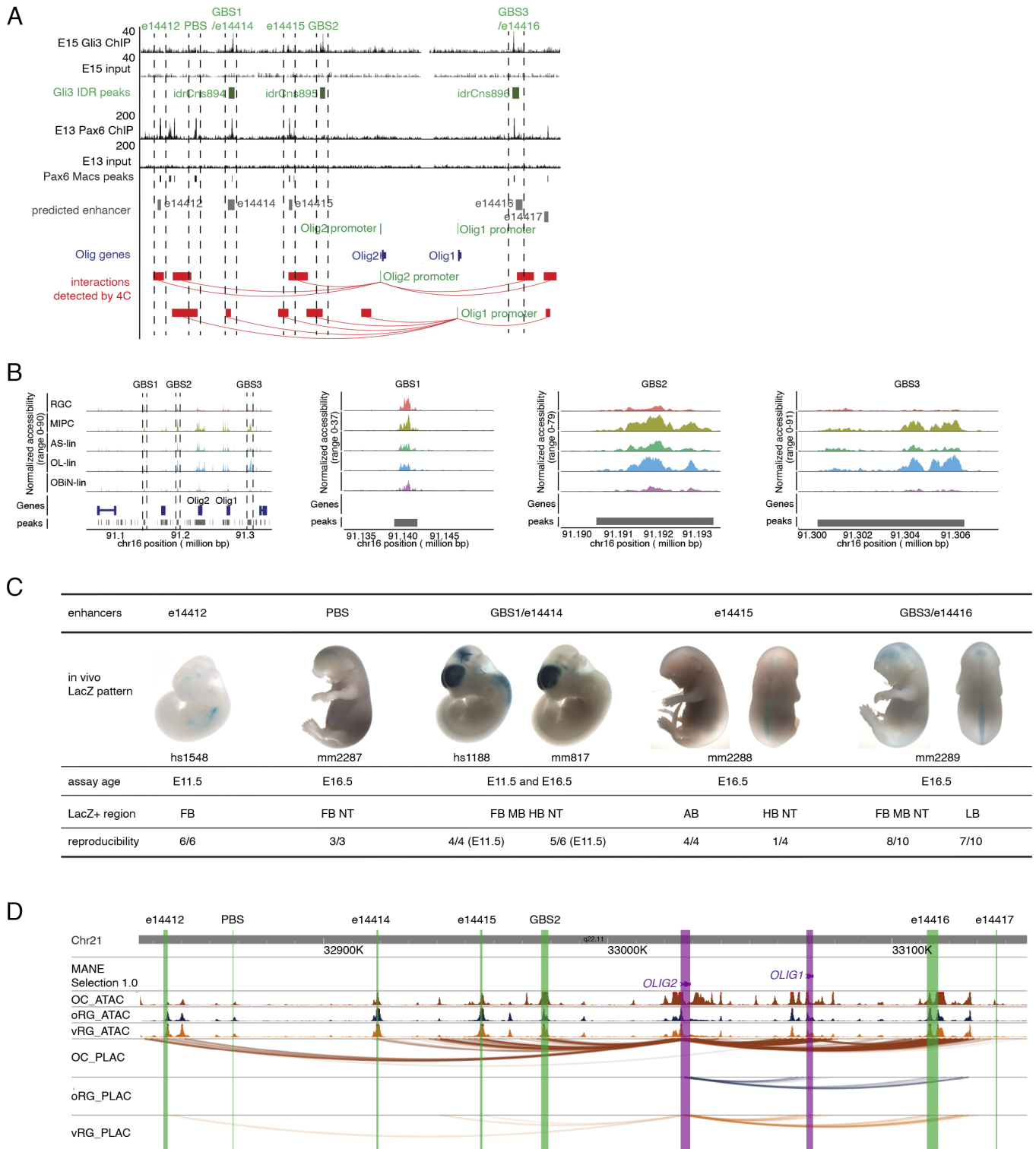


Fig. 4. Gli3 and Pax6 binding sites in the *Olig1/2* loci have enhancer activity and their interactions with the *Olig1/2* promoters are conserved between the mouse and human. (A) ChIP-seq analysis showed Gli3 binds to three sites in the *Olig1/2* loci (GBS1/e14414, GBS2, and GB3/e14416), and Pax6 binds to multiple sites including e14412, PBS, e14414, e14415, and e14416. The e14412, e14414, e14415, e14416, and e14417 are enhancers predicted by the ENCODE project, and are shown in gray. The red blocks represent the regions that interacted with *Olig2* or *Olig1* promoters in the cortical cells, as revealed in the 4C experiments. Note that GBS1 is part of e14414, and GBS3 overlaps with e14416. (B) Single-cell ATAC-seq revealed that the 3 GBS sequences are differentially accessible in RGCs, MIPCs, astrocyte, oligodendrocyte, and olfactory bulb interneuron lineages. (C) Enhancer reporter assays showed that the Gli3 and Pax6 binding sites have enhancer activity in E11.5 or E16.5 mouse embryos. Note that hs1528 (e14412) and hs1188 (e14414) are human sequences, and mm817 is the mouse sequence for e14414. All the enhancer data have been loaded in the Vista Enhancer browser: mm2287 (PBS), mm2288 (e14415), and mm2289 (e14416). Abbreviations: FB, forebrain; NT, neural tube; MB, midbrain; HB, hindbrain; AB, abdomen; LB, limb. (D) H3K4me3 PLAC-seq experiments revealed that the Gli3 and Pax6 binding sites interact with *OLIG1* and *OLIG2* promoters in human fetal cortical glial lineage cells. The *OLIG1* and *OLIG2* promoters are shown in pink bars, the green bars represent the homologous sequences of the Gli3 and Pax6 binding peaks in human cells, and the wavy lines represent the interactions detected in H3K4me3 PLAC-seq. ATAC peaks in OC, oRG, and vRG cells are also shown. OC, glial lineage cells; oRG, outer radial glial cells; vRG, ventricular radial glial cells.

(SI Appendix, Fig. S7). In the *Olig2*^{Δe14414/Δe14414}, *Olig2*^{ΔGBS2/ΔGBS2}, and *Olig2*^{Δe14415/Δe14415} mice, *Olig2*⁺ and *Olig1*⁺ cell numbers in the cortical VZ/SVZ were reduced, while their numbers were not significantly affected in the *Olig2*^{Δe14416/Δe14416} mice (SI Appendix, Fig. S7). To circumvent effects of potential secondary mutations carried by the enhancer deletion alleles, we bred mice carrying enhancer deletion alleles to mice carrying an *Olig2* null allele (*Olig2*^{-/-}) (24) and analyzed brains from trans-heterozygous mice carrying one copy of an enhancer deletion allele and one copy of the *Olig2*^{-/-} allele. We compared the trans-heterozygotes to the *Olig2*^{+/-} and *Olig2*^{-/-} mice (Fig. 5). We found that *Olig2*⁺ cells were present in the VZ/SVZ and cortical plate in the *Olig2*^{+/-}, *Olig2*^{Δe14414}, *Olig2*^{Δe14415}, *Olig2*^{ΔGBS2}, and the *Olig2*^{Δe14416} mice (Fig. 5 C, G, K, O, and S), and absent in the *Olig2*^{-/-} mice

(Fig. 5W). Compared to the *Olig2*^{+/-} mice, the numbers of *Olig2*⁺ cells in the VZ/SVZ were significantly reduced in the *Olig2*^{-/Δe14414} and *Olig2*^{-/ΔGBS2} mice, but not in the *Olig2*^{-/Δe14415} and *Olig2*^{-/Δe14416} mice (Fig. 5Y), indicating that e14414 and GBS2, but not e14415 or e14416, are essential for efficient *Olig2* expression in the cortical progenitor cells. Similarly, the numbers of *Olig1*⁺ cells in the VZ/SVZ were reduced in both *Olig2*^{-/Δe14414} and *Olig2*^{-/ΔGBS2} mice (Fig. 5 D, H, P, and Z).

Olig2 is expressed in the lateral and medial VZ/SVZ, as well as the ventral VZ/SVZ. We observed reduced numbers of *Olig2*⁺ cells in the lateral, but not medial or ventral VZ/SVZ in the *Olig2*^{-/Δe14414} and *Olig2*^{Δe14414/Δe14414} mice (SI Appendix, Fig. S8). *Olig2* expression in the lateral, medial, or ventral VZ/SVZ was not affected in the *Olig2*^{Δe14415/Δe14415}, *Olig2*^{ΔGBS2/ΔGBS2}, or the

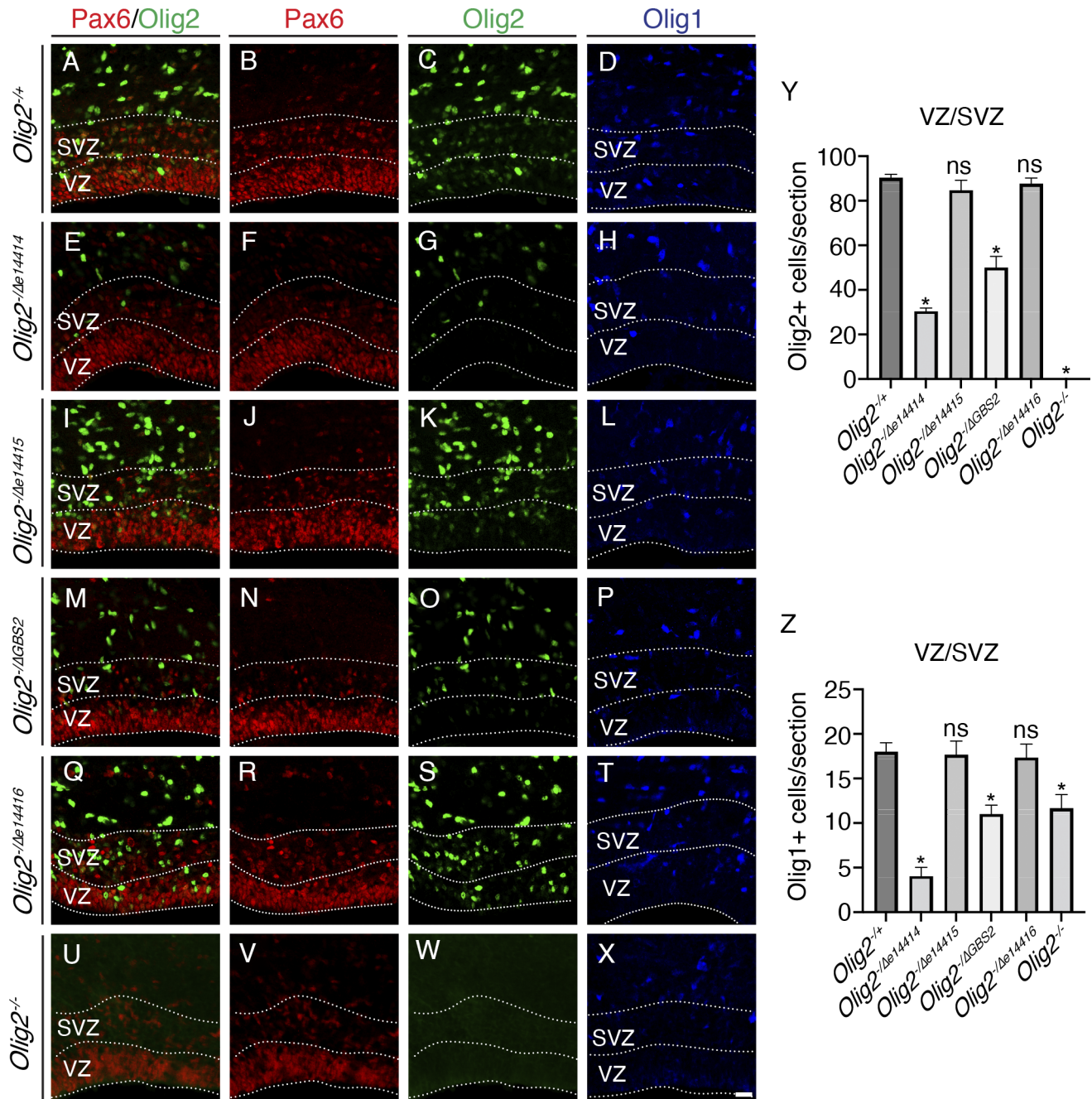


Fig. 5. Enhancers e14414 and GBS2 regulate *Olig2* and *Olig1* expression in cortical VZ/SVZ. P0 images were shown. (A–X) Immunostaining for Pax6, *Olig2*, *Olig1* in *Olig2*^{+/-} (A–D), *Olig2*^{-/Δe14414} (E–H), *Olig2*^{-/Δe14415} (I–L), *Olig2*^{-/ΔGBS2} (M–P), *Olig2*^{-/Δe14416} (Q–T), and *Olig2*^{-/-} (U–X) cortices. Pax6 expression delineates the VZ and SVZ. Images were taken at the rostral-middle position along the rostral-caudal axis. (Y and Z) Quantification *Olig2*⁺ and *Olig1*⁺ cells in 350-μm wide cortical VZ/SVZ regions. Numbers represent means + SEM (n = 3 mice per genotype). *P < 0.05; unpaired Student's t test. (Scale bar: 20 μm in X, applies to A–X.)

Olig2^{Δe14416/Δe14416} mice (*SI Appendix, Fig. S8*). Thus, e14414 regulates *Olig2* expression in the lateral VZ/SVZ.

We determined whether deletion of any of these enhancers affected gliogenesis or OB interneuron production in the cortex

using markers for glial progenitors, OB interneuron progenitors, and immature OB interneurons (Fig. 6). At P0, the *Olig2*⁺, *Olig1*⁺, *Egfr*⁺, and *Sox9*⁺ cells in the cortical plates are glial progenitors that can generate both astrocytes and oligodendrocytes.

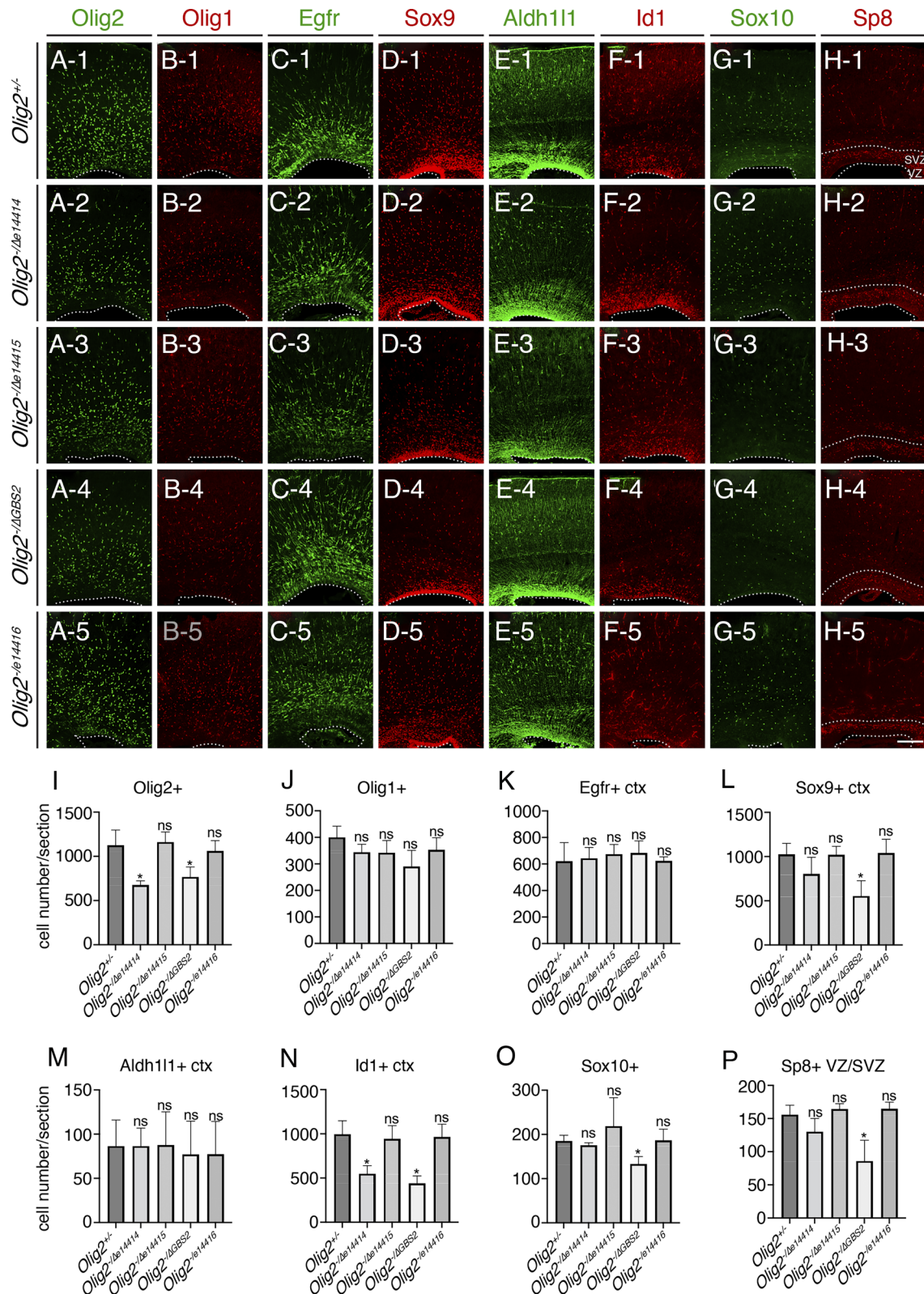


Fig. 6. Deletion of e14414 or GBS2 leads to defective lineage switch in the cortex. P0 images were shown. (A–H) Immunostaining for *Olig2* (A-1 to A-5), *Olig1* (B-1 to B-5), *Egfr* (C-1 to C-5), *Sox9* (D-1 to D-5), *Aldh111* (E-1 to E-5), *Id1* (F-1 to F-5), *Sox10* (G-1 to G-5), and *Sp8* (H-1 to H-5) in the cortices of *Olig2*^{+/+} (A-1 to H-1), *Olig2*^{-Δe14414} (A-2 to H-2), *Olig2*^{-Δe14415} (A-3 to H-3), *Olig2*^{-ΔGBS2} (A-4 to H-4), and *Olig2*^{-Δe14416} (A-5 to H-5) mice. Images were taken at the rostral-middle position along the rostral-caudal axis. (I–P) Quantification *Olig2*⁺, *Olig1*⁺, *Egfr*⁺, *Sox9*⁺, *Aldh111*⁺, *Id1*⁺, *Sox10*⁺, and *Sp8*⁺ cells. Numbers represent means + SEM (n = 3 mice per genotype). *P < 0.05; unpaired Student's *t* test. (Scale bar: 100 μm in H-5, applies to A-1 to H-5.)

Compared to the *Olig2*^{+/-} mice, the numbers of *Olig2*⁺ cells in the cortical plate were significantly reduced in the *Olig2*^{-/Δe14414} and *Olig2*^{-/ΔGBS2} mice, but not in the *Olig2*^{-/Δe14415} or *Olig2*^{-/Δe14416} mice (Fig. 6J). The numbers of Sox9⁺ cells were decreased in the cortical plate of the *Olig2*^{-/ΔGBS2} mice (Fig. 6L), while the numbers of *Olig1*⁺ and *Egfr*⁺ cells in the cortical plate were not significantly affected in the enhancer trans-heterozygous deletion mice (Fig. 6J and K). *Aldh111* and *Id1* are mostly expressed in astrocyte progenitors in the cortical plate at P0. *Aldh111*⁺ cells in the cortical plate in the enhancer trans-heterozygous deletion mice were not significantly different from those in the *Olig2*^{+/-} mice (Fig. 6M), while the *Id1*⁺ cells in the cortical plate showed a significant reduction in the *Olig2*^{-/Δe14414} and *Olig2*^{-/ΔGBS2} mice (Fig. 6N). There were fewer Sox10⁺ oligodendrocyte precursor cells in the cortical plate in the *Olig2*^{-/ΔGBS2} mice, but not in other enhancer trans-heterozygous deletion mice (Fig. 6O). Sp8 expression marks the OB interneuron progenitors and immature OB interneurons in the cortical VZ/SVZ. Compared to the *Olig2*^{+/-} mice, the numbers of Sp8⁺ OB interneuron precursors were significantly reduced in the *Olig2*^{-/ΔGBS2} mice (Fig. 6P). Together, these results indicate that enhancers e14414 and GBS2 are both required for efficient expression of *Olig2* in the cortical progenitors, while deletion of e14414 reduced the *Id1*⁺ glial progenitors, and deletion of GBS2 reduced the progenitors for both types of cortical macroglia and olfactory bulb interneuron precursors. Thus, GBS2 is essential for cortical gliogenesis and OB interneuron production.

Discussion

At the end of cortical excitatory neuron production, cortical RGCs switch lineage to generate astrocytes, oligodendrocytes, and OB interneurons (3–6, 10, 12). Some late cortical RGCs migrate away from the VZ into the cortical plate; they become translocating RGCs that produce astrocytes. Other late RGCs divide at VZ and generate transient *Ascl1*⁺*Egfr*⁺*Olig2*⁺ MIPCs; these MIPCs divide and generate the progenitors for cortical astrocytes, oligodendrocytes, and inhibitory OB interneurons (12, 13). Immunohistochemical and scRNA-seq data analyses revealed the presence of *Ascl1*⁺*Egfr*⁺*Olig2*⁺ MIPCs in the cortical VZ/SVZ of fetal human brains, which give rise to intermediate progenitors for both cortical macroglia and OB interneurons (13). This indicates that the generation of *Ascl1*⁺*Egfr*⁺*Olig2*⁺ cortical MIPCs and activating expression of *Egfr* and *Olig2* in cortical progenitors are conserved during mammalian brain development.

Recent elegant studies revealed the important functions of *Egfr* in regulating cortical gliogenesis (5, 6). Using mosaic analysis with double markers (MADM) to sparsely delete *Egfr* in cortical progenitors, Zhang et al. showed *Egfr* to be required in rostradorsal, but not ventrocaudal glial lineages (5, 6). Lineage analysis of *Olig2*⁺ cortical progenitors indicated that they give rise to OB interneurons, cortical oligodendrocytes, and almost all the cortical astrocytes (12). Expression of *Olig2* in the cortical progenitors is essential for cortical RGCs to generate astrocytes and oligodendrocytes (18, 21). During mouse embryonic and human fetal brain development, both *Egfr/EGFR* and *Olig2/OLIG2* are initially expressed in the VZ/SVZ of the ventral forebrain and start to be expressed in the cortical VZ/SVZ as cortical RGCs start to generate glial and OB interneuron lineages (12, 13). How *Egfr/EGFR* and *Olig2/OLIG2* become transcriptionally activated in cortical progenitors has remained unexplored.

In this study, we showed that expression of both *Egfr* and *Olig2* in cortical progenitors is under the control of Shh signaling. We focused on how the transcription of *Olig2* is regulated in cortical progenitors by identifying its cortical enhancers. We showed that

Gli3 and *Pax6*, two transcription factors highly expressed in cortical RGCs, inhibit *Olig2* expression. By performing ChIP and CUT&RUN experiments and examining previously published *Pax6* ChIP-seq data (35), we showed that both *Gli3* and *Pax6* bind to multiple sites in the *Olig1/2* loci (Fig. 4A and *SI Appendix, Fig. S6*). Results from CUT&RUN experiments using antibodies for H3K4me3, H3K27me3, and H3K27ac as well as bulk ATAC-seq and single-cell ATAC-seq experiments suggested that the *Gli3* and *Pax6* binding sites in the *Olig1/2* loci were potential enhancers (Fig. 4A and B and *SI Appendix, Fig. S6*). 4C experiments showed that *Gli3* and *Pax6* binding sites interacted with *Olig1/2* promoters in the developing cortex (Fig. 4A). Transgenic reporter mice showed that e14412, PBS, e14414/GBS1, e14415, and e14416/GBS3 had enhancer activity (Fig. 4B), and some of them were active in the developing forebrain (Fig. 4B). By generating enhancer knockout mice, we showed that both e14414/GBS1 and GBS2 are essential for efficient *Olig2* expression in the cortical progenitors, and are required for proper generation of glial progenitors in the developing cortex (Figs. 5 and 6). Thus, we have identified critical enhancer sequences for *Olig2* transcriptional regulation.

Cortical RGC lineage switch ensures proper numbers of neuronal and glial cell types are generated, and it is a conserved, but incompletely understood, feature in mouse and human cortical development (12, 13). Similar to the mouse brain, *OLIG2* expression begins in the human cortical SVZ when cortical progenitors start to generate glial lineages in the fetal brain (13). We found that the sequences of *Gli3* and *Pax6* binding sites are conserved in the human genome, and they interact with the *OLIG2* and *OLIG1* promoters in the cortical progenitor cells and glial lineages in the fetal brain (Fig. 4D). Similar to the mouse e14414/mm817 sequence, the homologous human sequence hs1188 drives strong *LacZ* expression in the mouse embryonic cortex (Fig. 4C). These results reveal conserved regulatory logic for *OLIG2* expression during human brain development.

Although we have identified critical enhancers that regulate *Olig2* expression in cortical progenitors, the molecular mechanism for how *Egfr* is transcriptionally activated by Shh and other signaling pathways remains to be determined. Interestingly, while Shh signaling is required across the rostro-caudal and medial-lateral axes of the cortical VZ/SVZ to activate *Olig2* and *Egfr* expression, *Egfr* regulates cortical gliogenesis in a regional-dependent manner (5, 6). Given that the MAPK pathway is strictly required for cortical gliogenesis (25), it is likely that signal transduction pathways other than the *Egfr* signaling activate the MAPK pathway in the ventrocaudal cortical regions.

Oligodendrocytes in the cerebral cortex originate from multiple sources (41). Although *Ascl1*⁺*Egfr*⁺*Olig2*⁺ MIPCs and *Olig2*⁺ Sox10⁺ OPCs are reduced in the cortices of *Smo* *cko* around birth, the numbers of OPCs and oligodendrocytes partially recover over time during later developmental stages (42). Both the expansion of ventrally derived OPCs and the proliferation of remaining cortical-derived OPCs contribute to this partial recovery (42). Future study should address the mechanisms by which the cortical RGCs generate OPCs and oligodendrocytes in the absence of Shh signaling.

Materials and Methods

Experiments were performed according to protocols approved by the Institutional Animal Care and Use Committee at University of California at Santa Cruz, University of South Dakota Sanford School of Medicine, and Lawrence Berkeley National Laboratory. Deidentified fetal tissue samples were collected with prior informed consent in strict observance of legal and institutional ethical

regulations. All protocols were approved by the Human Gamete, Embryo, and Stem Cell Research Committee and Institutional Review Board at the University of California, San Francisco.

Generation of *Olig2*^{Δ^{e14415/+}}, *Olig2*^{Δ^{GBS2/+}}, and *Olig2*^{Δ^{e14416/+}} mice: These mice were generated using the iGONAD method (43), using two guide RNAs and a HDR donor oligo as repair template for each enhancer. Detailed information can be found in *SI Appendix*.

Generation of the enhancer reporter mice: These mice were generated and analyzed as described previously (36–38). Detailed information can be found in *SI Appendix*.

Immunohistochemistry, ChIP-seq, CUT&RUN, ATAC-seq, 4C, in utero electroporation (IUE), H3K4me3-PLAC-seq, western blot, quantification, and statistical analysis were performed according to published protocols. Information for the mouse lines used and generated, detailed experimental procedures, and analyses can be found in *SI Appendix*.

Data, Materials, and Software Availability. ChIP-seq, CUT&RUN, and ATAC-seq generated in this study have been deposited in the Gene Expression Omnibus (GEO) under the accession number [GSE254693](https://www.ncbi.nlm.nih.gov/geo/query/acc.cgi?acc=GSE254693) (28).

1. D. P. Leone, K. Srinivasan, B. Chen, E. Alcamo, S. K. McConnell, The determination of projection neuron identity in the developing cerebral cortex. *Curr. Opin. Neurobiol.* **18**, 28–35 (2008).
2. M. J. Eckler *et al.*, Cux2-positive radial glial cells generate diverse subtypes of neocortical projection neurons and macroglia. *Neuron* **86**, 1100–1108 (2015).
3. L. C. Fuentealba *et al.*, Embryonic origin of postnatal neural stem cells. *Cell* **161**, 1644–1655 (2015).
4. Y. Zhang *et al.*, Cortical neural stem cell lineage progression is regulated by extrinsic signaling molecule sonic hedgehog. *Cell Rep.* **30**, 4490–4504 (2020).
5. X. Zhang *et al.*, Clonal analysis of gliogenesis in the cerebral cortex reveals stochastic expansion of glia and cell autonomous responses to Egfr dosage. *Cells* **9**, 2662 (2020).
6. X. Zhang *et al.*, Bulk and mosaic deletions of Egfr reveal regionally defined gliogenesis in the developing mouse forebrain. *iScience* **26**, 106242 (2023).
7. Q. Shen *et al.*, The timing of cortical neurogenesis is encoded within lineages of individual progenitor cells. *Nat. Neurosci.* **9**, 743–751 (2006).
8. S. J. Franco *et al.*, Fate-restricted neural progenitors in the mammalian cerebral cortex. *Science* **337**, 746–749 (2012).
9. C. Guo *et al.*, Fez2 expression identifies a multipotent progenitor for neocortical projection neurons, astrocytes, and oligodendrocytes. *Neuron* **80**, 1167–1174 (2013).
10. P. Gao *et al.*, Deterministic progenitor behavior and unitary production of neurons in the neocortex. *Cell* **159**, 775–1788 (2014).
11. C. Gil-Sanz *et al.*, Lineage tracing using Cux2-Cre and Cux2-CreERT2 mice. *Neuron* **86**, 1091–1099 (2015).
12. X. Li *et al.*, Decoding cortical glial cell development. *Neurosci. Bull.* **37**, 440–460 (2021).
13. L. Yang, Z. Li, G. Liu, X. Li, Z. Yang, Developmental origins of human cortical oligodendrocytes and astrocytes. *Neurosci. Bull.* **38**, 47–68 (2022).
14. C. M. Parras *et al.*, Mash1 specifies neurons and oligodendrocytes in the postnatal brain. *EMBO J.* **23**, 4495–4505 (2004).
15. C. M. Parras *et al.*, The proneural gene Mash1 specifies an early population of telencephalic oligodendrocytes. *J. Neurosci.* **27**, 4233–4242 (2007).
16. T. Y. Yue, E. J. Kim, C. M. Parras, F. Guillemot, J. E. Johnson, Ascl1 controls the number and distribution of astrocytes and oligodendrocytes in the gray matter and white matter of the spinal cord. *Development* **141**, 3721–3731 (2014).
17. D. J. Dennis *et al.*, Neurog2 and Ascl1 together regulate a postmitotic derepression circuit to govern laminar fate specification in the murine neocortex. *Proc. Natl. Acad. Sci. U.S.A.* **114**, E4934–E4943 (2017).
18. C. A. Marshall, B. G. Novitsch, J. E. Goldman, Olig2 directs astrocyte and oligodendrocyte formation in postnatal subventricular zone cells. *J. Neurosci.* **25**, 7289–7298 (2005).
19. W. Liu *et al.*, Disruption of neurogenesis and cortical development in transgenic mice misexpressing Olig2, a gene in the Down syndrome critical region. *Neurobiol. Dis.* **77**, 106–116 (2015).
20. K. Ono *et al.*, Regional- and temporal-dependent changes in the differentiation of Olig2 progenitors in the forebrain, and the impact on astrocyte development in the dorsal pallidum. *Dev. Biol.* **320**, 456–468 (2008).
21. J. Cai *et al.*, A crucial role for Olig2 in white matter astrocyte development. *Development* **134**, 1887–1899 (2007).
22. C. C. Winkler *et al.*, The dorsal wave of neocortical oligodendrogenesis begins embryonically and requires multiple sources of sonic hedgehog. *J. Neurosci.* **38**, 5237–5250 (2018).
23. F. Long, X. M. Zhang, S. Karp, Y. Yang, A. P. McMahon, Genetic manipulation of hedgehog signaling in the endochondral skeleton reveals a direct role in the regulation of chondrocyte proliferation. *Development* **128**, 5099–5108 (2001).
24. M. Zawadzka *et al.*, CNS-resident glial progenitor/stem cells produce Schwann cells as well as oligodendrocytes during repair of CNS demyelination. *Cell Stem Cell* **6**, 578–590 (2010).
25. X. Li *et al.*, MEK is a key regulator of gliogenesis in the developing brain. *Neuron* **75**, 1035–1050 (2012).
26. E. S. Jang, J. E. Goldman, Pax6 expression is sufficient to induce a neurogenic fate in glial progenitors of the neonatal subventricular zone. *PLoS One* **6**, e20894 (2011).
27. A. Stoykova, D. Treichel, M. Hallonet, P. Gruss, Pax6 modulates the dorsoventral patterning of the mammalian telencephalon. *J. Neurosci.* **20**, 8042–8050 (2000).
28. X. G. Liang *et al.*, A conserved molecular logic for neurogenesis to gliogenesis switch in the cerebral cortex. *NCBI Gene Expression Omnibus*. <https://www.ncbi.nlm.nih.gov/geo/query/acc.cgi?acc=GSE254693#>. Deposited 31 January 2024.
29. Q. H. Li, J. B. Brown, H. Y. Huang, P. J. Bickel, Measuring reproducibility of high-throughput experiments. *Ann. Appl. Stat.* **5**, 1752–1779 (2011).
30. D. U. Gorkin *et al.*, An atlas of dynamic chromatin landscapes in mouse fetal development. *Nature* **583**, 744–751 (2020).
31. C. A. Sloan *et al.*, ENCODE data at the ENCODE portal. *Nucleic Acids Res.* **44**, D726–D732 (2016).
32. J. R. Dixon *et al.*, Topological domains in mammalian genomes identified by analysis of chromatin interactions. *Nature* **485**, 376–380 (2012).
33. P. H. L. Krijger, G. Geeven, V. Bianchi, C. R. E. Hilvering, W. de Laat, 4C-seq from beginning to end: A detailed protocol for sample preparation and data analysis. *Methods* **170**, 17–32 (2020).
34. L. Zhuo *et al.*, Live astrocytes visualized by green fluorescent protein in transgenic mice. *Dev. Biol.* **187**, 36–42 (1997).
35. A. R. Ypsilanti *et al.*, Transcriptional network orchestrating regional patterning of cortical progenitors. *Proc. Natl. Acad. Sci. U.S.A.* **118**, e2024795118 (2021).
36. A. Visel, S. Minovitsky, I. Dubchak, L. A. Pennacchio, VISTA Enhancer Browser—A database of tissue-specific human enhancers. *Nucleic Acids Res.* **35**, D88–D92 (2007).
37. E. Z. Kvon *et al.*, Comprehensive in vivo interrogation reveals phenotypic impact of human enhancer variants. *Cell* **180**, 1262–1271.e15 (2020).
38. M. Osterwalder *et al.*, Characterization of mammalian in vivo enhancers using mouse transgenesis and CRISPR genome editing. *Methods Mol. Biol.* **2403**, 147–186 (2022).
39. M. Song *et al.*, Cell-type-specific 3D epigenomes in the developing human cortex. *Nature* **587**, 644–649 (2020).
40. S. F. Altschul, W. Gish, W. Miller, E. W. Myers, D. J. Lipman, Basic local alignment search tool. *J. Mol. Biol.* **215**, 403–410 (1990).
41. N. Kessarar *et al.*, Competing waves of oligodendrocytes in the forebrain and postnatal elimination of an embryonic lineage. *Nat. Neurosci.* **9**, 173–179 (2006).
42. C. C. Winkler, S. J. Franco, Loss of Shh signaling in the neocortex reveals heterogeneous cell recovery responses from distinct oligodendrocyte populations. *Dev. Biol.* **452**, 55–65 (2019).
43. Y. Imai, A. Tanave, M. Matsuyama, T. Koide, Efficient genome editing in wild strains of mice using the i-GONAD method. *Sci. Rep.* **12**, 13821 (2022).